Free Radical Biology & Medicine 48 (2010) 1109–1117

Contents lists available at ScienceDirect

Free Radical Biology & Medicine

journal homepage: www.elsevier.com/locate/freeradbiomed

Original Contribution

Protection of podocytes from hyperhomocysteinemia-induced injury by deletion of the gp91^{phox} gene

Chun Zhang, Jun-Jun Hu, Min Xia, Krishna M. Boini, Christopher A. Brimson, Laura A. Laperle, Pin-Lan Li *

Department of Pharmacology & Toxicology, Medical College of Virginia, Virginia Commonwealth University, Richmond, VA 23298, USA

ARTICLE INFO

Article history:
Received 21 September 2009
Revised 12 January 2010
Accepted 21 January 2010
Available online 29 January 2010

Keywords:
Homocysteinemia
Glomerulosclerosis
Glomerulus
Redox signaling
Free radicals

ABSTRACT

In this study, mice lacking the gp91^{phox} gene were used to address the role of NADPH oxidase in hyperhomocysteinemia-induced podocyte injury. It was found that a folate-free diet increased plasma homocysteine levels, but failed to increase $O_2^{\bullet-}$ production in the glomeruli from gp91^{phox} gene knockout (gp91$^{-/-}$) mice, compared with wild-type (gp91$^{+/+}$) mice. Proteinuria and glomerular damage index (GDI) were significantly lower, whereas the glomerular filtration rate (GFR) was higher in gp91$^{-/-}$ than in gp91$^{+/+}$ mice when they were on the folate-free diet (urine albumin excretion, 21.23 ± 1.88 vs 32.86 ± 4.03 μg/24 h; GDI, 1.17 ± 0.18 vs 2.59 ± 0.49; and GFR, 53.01 ± 4.69 vs 40.98 ± 1.44 μl/min). Hyperhomocysteinemia-induced decrease in nephrin expression and increase in desmin expression in gp91$^{+/+}$ mice were not observed in gp91$^{-/-}$ mice. Morphologically, foot process effacement and podocyte loss due to hyperhomocysteinemia were significantly attenuated in gp91$^{-/-}$ mice. In in vitro studies of podocytes, homocysteine was found to increase gp91^{phox} expression and $O_2^{\bullet-}$ generation, which was substantially inhibited by gp91^{phox} siRNA. Functionally, homocysteine-induced decrease in vascular endothelial growth factor-A production was abolished by gp91^{phox} siRNA or diphenyleneiodonium, a NADPH oxidase inhibitor. These results suggest that the functional integrity of NADPH oxidase is essential for hyperhomocysteinemia-induced podocyte injury and glomerulosclerosis.

Hyperhomocysteinemia (hHcys) has been known as a critical pathogenic factor both in the progression of end-stage renal disease (ESRD) and in the development of cardiovascular complications related to ESRD [1–3]. It has been reported that sustained hHcys may induce extracellular matrix accumulation and inhibit their degradation in the kidney, which ultimately leads to glomerulosclerosis [4]. Although many downstream signaling pathways are involved in hHcys-induced glomerulosclerosis, reactive oxygen species (ROS) are currently regarded as one of the most important mediators in the initiation of hHcys-induced kidney damage. Among ROS, superoxide ($O_2^{\bullet-}$) is a main source for other oxygen-centered radicals, such as H_2O_2 and $^{\bullet}OH$, which participate in lipid peroxidation and induce cellular membrane damage. Emerging evidence has highlighted the important role for the nicotinamide adenine dinucleotide phosphate (NADPH) oxidase-dependent system as a major source of $O_2^{\bullet-}$ in the kidney [5]. Recently, we and others have shown that NADPH oxidase activation and subsequent $O_2^{\bullet-}$ generation are important mechanisms in the development of hHcys-induced glomerulosclerosis [6,7].

NADPH oxidase comprises the membrane-bound cytochrome b_{558} (formed by gp91^{phox} and p22^{phox} subunits) and the cytosolic proteins p40^{phox}, p47^{phox}, p67^{phox}, and Rac1/2. The catalytic subunits of this enzyme are termed NOX proteins, which include NOX1, NOX2 (i.e., gp91^{phox}), NOX3, NOX4, NOX5, DUOX1, and DUOX2 [8]. It has been reported that almost all components of the NADPH oxidase complex, including gp91^{phox}, p22^{phox}, p47^{phox}, p67^{phox}, and Rac1/2, are expressed in the kidney and that these NADPH oxidase components could be detected in renal fibroblasts, endothelial cells, vascular smooth muscle cells, mesangial cells, and tubular cells [9]. Among these, the catalytic subunit gp91^{phox} was shown to be essential for oxidative stress in the kidney. Previous studies using gp91^{phox} knockout mice have demonstrated that this enzyme plays important roles in the maintenance of renal vascular tone [10], as well as in the regulation of renal hemodynamics and excretory function under a condition of nitric oxide deficiency [11]. Recently, several NADPH oxidase subunits, gp91^{phox}, p22^{phox}, p67^{phox}, and p47^{phox}, have been also demonstrated to be present in cultured podocytes [12]. Further studies showed that NADPH oxidase activation and subsequent $O_2^{\bullet-}$ production play a key role in high glucose-, angiotensin II-, and adriamycin-induced podocyte injury [13–15]. However, it remains unknown whether activation of NADPH oxidase is involved in hHcys-induced podocyte injury and related pathological changes.

Podocytes are terminally differentiated epithelial cells, which cover the outermost layer of glomerular filtration barrier and constitute the last and the most important barrier in preventing protein leakage from the plasma. Although podocyte injury has been considered as the most important early event in initiating glomerulosclerosis and thereby

* Corresponding author. Fax: +1 804 828 4794.
E-mail address: pli@vcu.edu (P.-L. Li).

0891-5849/$ – see front matter © 2010 Elsevier Inc. All rights reserved.
doi:10.1016/j.freeradbiomed.2010.01.029

resulting in ESRD in various animal models and humans [16–18], its involvement in hHcys-induced glomerular damage and sclerosis is still poorly understood. We hypothesized that homocysteine (Hcys) may directly cause podocyte injury through NADPH oxidase-mediated $O_2^{\bullet-}$ production and that knockout or deletion of its functional subunit, gp91^{phox}, will protect podocytes from hHcys-induced injury. To test this hypothesis, we determined the possible injurious effect of hHcys on podocytes in mice lacking the gp91^{phox} gene and compared related pathological changes to their genetic background strain C57BL/6 mice. We further used cultured murine podocytes to examine the direct effects of gp91^{phox} gene deletion on Hcys-induced functional changes in podocytes and explored the underlying mechanisms.

Materials and methods

Animal procedures

C57BL/6J wild-type (WT; 6 weeks of age, male) and gp91^{phox} knockout (KO) mice (6 weeks of age, male; The Jackson Laboratory, Bar Harbor, ME, USA) were used. All protocols were approved by the Institutional Animal Care and Use Committee of the Virginia Commonwealth University. Given the difficulty of the development of hyperhomocysteinemia in mice with both kidneys because of treatment that requires a long period of time, all gp91^{phox} KO mice and WT mice were subjected to a uninephrectomy, which helped accelerate the progression of hHcys-induced glomerular injury, as we reported previously [6]. This model was demonstrated to induce glomerular damage unrelated to the uninephrectomy and arterial blood pressure, but specific to hHcys. After a 1-week recovery period from the uninephrectomy, KO and WT mice were fed a normal diet or a folate-free (FF) diet (Dyets, Inc., Bethlehem, PA, USA) for 4 weeks to induce hHcys. One day before these mice were sacrificed, 24-h urine samples were collected using mouse metabolic cages. After blood samples were collected, the mice were sacrificed and renal tissues were harvested for biochemical and molecular analysis as well as morphological examinations.

High-performance liquid chromatography (HPLC) analysis

Plasma total Hcys levels were measured by HPLC as we described previously [19]. Briefly, blood samples were centrifuged at 1000*g* for 10 min at 4°C to isolate the plasma. One hundred microliters of plasma, or standard solution mixed with 10 μl of internal standard, thionglycolic acid (2.0 mmol/L) solution, was treated with 10 μl of 10% tri-*n*-butylphosphine solution in dimethylformamide at 4°C for 30 min. Then, 80 μl of ice-cold 10% trichloroacetic acid in 1 mmol/L EDTA was added and centrifuged to remove proteins in the sample. One hundred microliters of the supernatant was transferred into the mixture of 20 μl of 1.55 mol/L sodium hydroxide, 250 μl of 0.125 mol/L borate buffer (pH 9.5), and 100 μl of 1.0 mg/ml ABD-F solution. The resulting mixture was incubated at 60°C for 30 min to accomplish derivatization of plasma thiols. HPLC was performed with an HP 1100 series equipped with a binary pump, a vacuum degasser, a thermostated column compartment, and an autosampler (Agilent Technologies, Waldbronn, Germany). Separation was carried out at ambient temperature on an analytical column, Supelco LC-18-DB (1504.6-mm i.d., 5 m) with a Supelcosil LC-18 guard column (204.6-mm i.d., 5 m). Fluorescence intensities were measured with an excitation wavelength of 385 nm and emission wavelength of 515 nm by a Hewlett–Packard Model 1046A fluorescence spectrophotometer. The peak area of the chromatographs was quantified with a Hewlett–Packard 3392 integrator. The analytical column was eluted with 0.1 mol/L potassium dihydrogen phosphate buffer (pH 2.1) containing 6% acetonitrile (v/v) as the mobile phase with a flow rate of 2.0 ml/min.

Monitoring of arterial blood pressure in conscious mice

Mean arterial pressure (MAP) was measured 4 weeks after mice were treated with the normal or FF diet as we described previously [20]. In brief, mice were anesthetized by inhalation of isoflurane, and then a catheter connected to a telemetry transmitter was implanted into the carotid artery and the transmitter was placed subcutaneously. The arterial blood pressure signal from the transmitter was received by a remote receiver and then recorded by a computer program (Data Sciences International, St. Paul, MN, USA). Arterial blood pressure was continuously measured for 1 week after an equilibration period.

Electromagnetic spin resonance (ESR) analysis of $O_2^{\bullet-}$ production

For detection of NADPH oxidase-dependent $O_2^{\bullet-}$ production, proteins from the isolated glomeruli of mice or cultured podocytes were extracted using sucrose buffer and resuspended with modified Krebs–Hepes buffer containing deferoximine (100 μmol/L; Sigma, St. Louis, MO, USA) and diethyldithiocarbamate (5 μmol/L; Sigma). NADPH oxidase-dependent $O_2^{\bullet-}$ production was examined in 50 μg of protein in the presence or absence of superoxide dismutase (200 U/ml; Sigma). The mixture was loaded in glass capillaries and immediately analyzed for $O_2^{\bullet-}$ production kinetically for 10 min in a Miniscope MS200 ESR spectrometer (Magnettech Ltd., Berlin, Germany) as we described for other studies [21,22]. The ESR settings were as follows: biofield, 3350; field sweep, 60 G; microwave frequency, 9.78 GHz; microwave power, 20 mW; modulation amplitude, 3 G; 4096 points of resolution; receiver gain, 20 for tissue and 50 for cells. The results were expressed as the fold changes of control.

Measurement of creatinine clearance (Ccr)

Plasma and urinary creatinine concentrations (Pcr and Ucr) were measured as described before [23]. In brief, 24-h urine samples were collected using metabolic cages. Blood samples for serum creatinine were collected at the time the mice were sacrificed. Serum and urinary creatinine concentrations were measured by a QuantiChrom creatinine assay kit (BioAssay Systems, Hayward, CA, USA). Ccr was calculated using the following formula: Ccr (μl/min) = (Ucr/Pcr) × urine volume (μl/min).

Urinary total protein and albumin excretion measurement

The 24-h urine samples were collected using metabolic cages and subjected to total protein and albumin excretion measurement, respectively. Total protein content in the urine was detected by the Bradford method using a UV spectrometer. Urine albumin was detected using a commercially available mouse albumin ELISA kit (Bethyl Laboratories, Montgomery, TX, USA).

Morphological examination

For observation of renal morphology using light microscopy, renal tissues were fixed with 10% formalin solution, paraffin-embedded, and stained with periodic acid–Schiff (PAS). Glomerular sclerosis was assessed by a standard semiquantitative analysis and expressed as glomerular damage index (GDI) [24]. Fifty glomeruli per slide were counted and graded as 0, 1, 2, 3, or 4, according to 0, <25, 25–50, 51–75, or >75% sclerotic changes across a longitudinal kidney section, respectively. The GDI for each mouse was calculated by the formula $((N_1\times1) + (N_2\times2) + (N_3\times3) + (N_4\times4))/n$, where N_1, N_2, N_3, and N_4 represent the numbers of glomeruli exhibiting grades 1, 2, 3, and 4, respectively, and n is the total number of glomeruli graded.

For transmission electron microscopic (TEM) observation of ultrastructural changes in podocytes, the kidneys were perfused with a fixative containing 3% glutaraldehyde and 4% paraformaldehyde

in 0.1 M phosphate buffer. The kidneys were sliced longitudinally and cortical strips were cut into 1-mm^3 tissue blocks, which were further fixed with 3% glutaraldehyde for 12 h. After dehydration with ethanol, the samples were embedded in Durcupan resin for ultrathin sectioning and TEM examinations by the VCU electron microscopy core facility.

Real-time reverse transcription polymerase chain reaction (RT-PCR)

Total RNA from isolated mouse glomeruli or cultured podocytes was extracted using TRIzol reagent (Invitrogen, Carlsbad, CA, USA) according to the protocol as described by the manufacturer. RNA samples were quantified by measurement of optic absorbance at 260 and 280 nm in a spectrophotometer. The concentrations of RNA were calculated according to A_{260}. Aliquots of total RNA (1 μg) from each sample were reverse-transcribed into cDNA according to the instructions of the first-strand cDNA synthesis kit manufacturer (Bio-Rad, Hercules, CA, USA). Equal amounts of the reverse-transcriptional products were subjected to PCR amplification using SYBR green as the fluorescence indicator on a Bio-Rad iCycler system (Bio-Rad). The mRNA levels of target genes were normalized to the β-actin mRNA levels. The primers used in this study were synthesized by Operon (Huntsville, AL, USA) and the sequences were $gp91^{phox}$, sense TGGCA CATCGATCCCTCACTGAAA, antisense GGTCACTGCATCTAAGGCAACCT; vascular endothelial growth factor-A (VEGF-A), sense CAATGAT-GAAGCCCTGGAG, antisense TCTCCTATGTGCTGGCTTTG; and β-actin, sense TCGCTGCGCTGGTCGTC, antisense GGCCTCGTCACCCACATAGGA.

Immunofluorescent staining and immunohistochemistry

Indirect immunofluorescent staining was performed using frozen slides of mouse kidneys. After fixation with acetone, the slides were incubated with rabbit anti-nephrin 1:100 (Abcam, Cambridge, MA, USA), rabbit anti-podocin 1:200 (Sigma), or rabbit anti-desmin 1:100 (BD Biosciences, San Jose, CA, USA), overnight, at 4°C. Then, the slides were washed and incubated with corresponding FITC-labeled secondary antibodies. Finally, the slides were washed, mounted, and subjected to fluorescence microscopy examination. The images were captured with a Spot CCD camera (Diagnostic Instruments, Sterling Heights, MI, USA). All exposure settings were kept constant for each group of kidneys.

Because WT1 (Wilms' tumor suppressor gene) is exclusively expressed by podocytes and not by other cell types in the glomeruli, podocyte numbers were counted in mouse glomeruli using immunohistochemistry staining for WT1 as reported previously [25]. Briefly, kidney sections from paraffin-embedded tissues were prepared at 4-μm thickness and stained by an antibody to WT1 (1:50 dilution; Abcam) using a routine immunohistochemistry procedure. After staining, 50 consecutive glomerular cross sections per mouse were randomly chosen and the positively stained podocytes were counted by an observer who was blinded to the sample identity. Six mice were analyzed for each group. The number of podocytes per glomerulus was calculated from podocyte density multiplied by the glomerular volume as described before [26].

Cell culture

A conditionally immortalized mouse podocyte cell line, kindly provided by Dr. P.E. Klotman (Division of Nephrology, Department of Medicine, Mount Sinai School of Medicine, New York, NY, USA), was cultured on collagen I-coated flasks or plates in RPMI 1640 medium supplemented with recombinant mouse interferon-γ at 33°C. After differentiating at 37°C for 10–14 days without interferon-γ, the podocytes were used for the proposed experiments. In this study, the preparation of L-Hcys (a pathogenic form of Hcys) and the concentration and incubation time of L-Hcys treatment were chosen based on our previous studies in mesangial cells [27] and our preliminary experiments on podocytes.

$Gp91^{phox}$ siRNA transfection

$Gp91^{phox}$ siRNA, purchased from Qiagen (Valencia, CA, USA), was confirmed to be effective in silencing the $gp91^{phox}$ gene in various cells by the company. The scrambled RNA (sRNA; Qiagen) was confirmed as nonsilencing double-stranded RNA and used as the control in this study. Podocytes were serum starved for 12 h and then transfected with $gp91^{phox}$ siRNA or sRNA using the siLentFect lipid reagent (Bio-Rad). After 18 h of incubation at 37°C, the medium was changed and L-Hcys (80 μmol/L) added into the medium for the indicated times.

ELISA for VEGF-A secretion in podocytes

After being transfected with $gp91^{phox}$ siRNA or sRNA, or pretreated with diphenyleneiodonium (DPI; a NADPH oxidase inhibitor), podocytes were incubated with L-Hcys (80 μmol/L) for 24 h. A relatively specific podocyte injury compound, puromycin aminonucleoside (PAN; 100 μg/ml), was used to treat cells for 24 h to serve as a positive control. The supernatant was collected for ELISA of VEGF-A using a commercially available kit (R&D Systems, Minneapolis, MN, USA).

Statistical analysis

All of the values are expressed as means ± SEM. Significant differences among multiple groups were examined using ANOVA followed by a Student–Newman–Keuls test. The χ^2 test was used to access the significance of ratio and percentage data. $P<0.05$ was considered statistically significant.

Results

Reduction of hHcys-induced $O_2^{\bullet-}$ production in $gp91^{phox}$ KO mice

As shown by HPLC analysis, plasma Hcys levels were similar in WT and $gp91^{phox}$ KO mice on the normal diet. FF diet treatment significantly increased plasma Hcys levels in both WT and $gp91^{phox}$ KO mice (Fig. 1A). ESR analysis showed that glomerular $O_2^{\bullet-}$ production was lower in KO mice than in WT mice on the normal diet. On the FF diet, glomerular $O_2^{\bullet-}$ production increased by 2.4-fold in WT mice. However, FF diet-induced $O_2^{\bullet-}$ production was much less in KO mice compared with WT mice (Figs. 1B and 1C).

Alleviation of glomerular injury in $gp91^{phox}$ KO mice on the FF diet

In parallel to the elevation in plasma Hcys levels, the 24-h urinary total protein and albumin excretion was significantly increased in WT mice on the FF diet. In $gp91^{phox}$ KO mice, however, a similar level of plasma Hcys caused much less urinary total protein and albumin excretion (Figs. 2A and 2B). By PAS staining, we observed a typical pathological change in glomerular sclerotic damage in WT mice on the FF diet (Fig. 3A). The average GDI was substantially higher in WT mice on the FF diet, but much less in $gp91^{phox}$ KO mice on the same diet ($P<0.05$, Fig. 3B). To evaluate the glomerular filtration rate (GFR) of these mice, Ccr was measured. It was found that FF diet treatment induced a decline in Ccr in WT mice, whereas the Ccr was mostly preserved in $gp91^{phox}$ KO mice on the same diet (Fig. 4A). To explore whether these renal functional and pathological changes were associated with elevation of arterial blood pressure, MAP was measured in conscious mice using telemetry. FF diet treatment had no effect on MAP in either WT or KO mice (Fig. 4B).

Expression of nephrin, podocin, and desmin in $gp91^{phox}$ KO and WT mice

Next we determined whether the protective effect of $gp91^{phox}$ gene knockout is associated with the protection of podocytes from

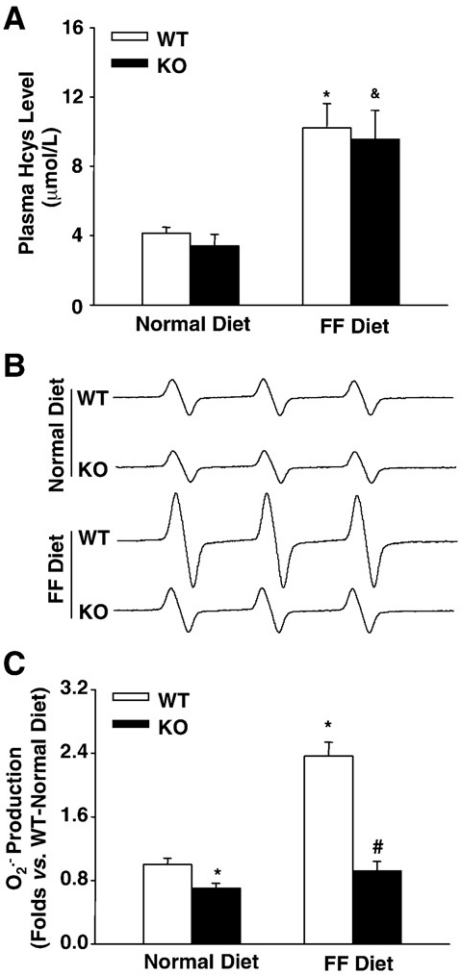

Fig. 1. Effects of normal and FF diets on plasma Hcys levels and glomerular $O_2^{\bullet-}$ production in gp91^{phox} KO and WT mice. (A) Plasma Hcys levels measured by HPLC in four groups of mice ($n=6$). (B) Representative ESR spectra traces for $O_2^{\bullet-}$ production in gp91^{phox} KO and WT mice ($n=5$). (C) Summarized data show the fold changes in $O_2^{\bullet-}$ production, which are normalized to WT mice on the normal diet ($n=5$). *$P<0.05$ vs WT mice on the normal diet; #$P<0.05$ vs WT mice on the FF diet; &$P<0.05$ vs KO mice on the normal diet.

hHcys-induced injury. Real-time RT-PCR demonstrated that the mRNA levels of two important slit diaphragm molecules, nephrin and podocin, were significantly decreased by the FF diet in WT mice, which decrease was much less in KO mice on the same diet. However, the expression of desmin, a podocyte injury marker, was significantly increased in WT mice on the FF diet compared with gp91^{phox} KO mice ($P<0.05$, Fig. 5A). As shown by indirect immunofluorescent staining in Fig. 5B, nephrin and podocin staining was seen as a fine linear-like pattern along the glomerular capillary loop in mice on a normal diet. The expression of both nephrin and podocin showed a dramatic decrease in WT mice on the FF diet, which was less obvious in the gp91^{phox} KO mice on the same diet. In contrast, the expression of desmin was less increased in gp91^{phox} KO mice on the FF diet compared with WT mice.

Attenuation of hHcys-induced foot process effacement and podocyte loss in gp91^{phox} KO mice

To observe ultrastructural changes in podocytes, TEM was conducted. Compared with the distinct brush-like structures of podocyte foot processes seen in mice on the normal diet, evident foot process effacement was observed in WT mice 4 weeks after FF diet treatment. In contrast, podocytes of gp91^{phox} KO mice on the FF diet had relatively normal ultrastructures (Fig. 6A). To investigate whether gp91^{phox} gene knockout helps to maintain podocyte numbers, we counted the number of podocytes per glomerular cross

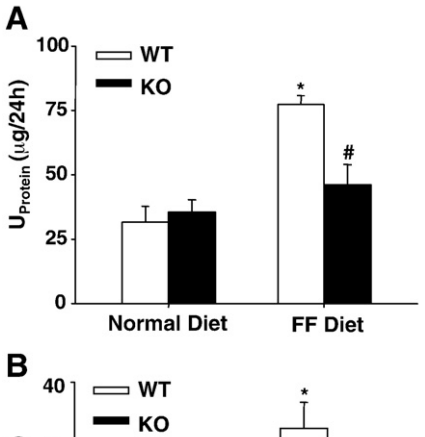

Fig. 2. Proteinuria was attenuated in gp91^{phox} KO mice on the FF diet. (A) Urinary total protein levels in the four groups of mice ($n=6$). (B) Urinary albumin excretion in the four groups of mice ($n=6$). *$P<0.05$ vs WT mice on the normal diet; #$P<0.05$ vs WT mice on the FF diet; &$P<0.05$ vs KO mice on the normal diet.

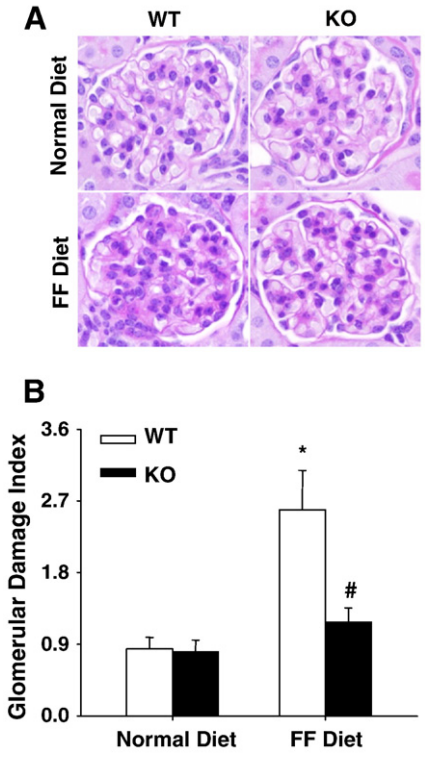

Fig. 3. Glomerular damage was alleviated in gp91^{phox} KO mice on the FF diet. (A) PAS staining shows glomerular morphological changes (original magnification, ×400). (B) Summarized data of GDI by semiquantitation of scores in the four groups of mice (for each group, $n=6$). For each kidney section, 50 glomeruli were randomly chosen for the calculation of GDI. *$P<0.05$ vs WT mice on the normal diet; #$P<0.05$ vs WT mice on the FF diet.

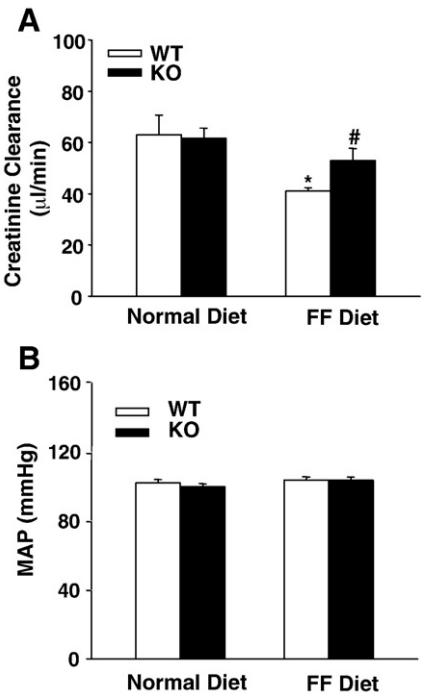

Fig. 4. Ccr and arterial blood pressure in gp91^{phox} KO and WT mice. (A) Creatinine clearance in WT and KO mice on a normal or FF diet ($n=7$). (B) MAP in WT and KO mice with or without FF diet ($n=5$). *$P<0.05$ vs WT mice on the normal diet; #$P<0.05$ vs WT mice on the FF diet.

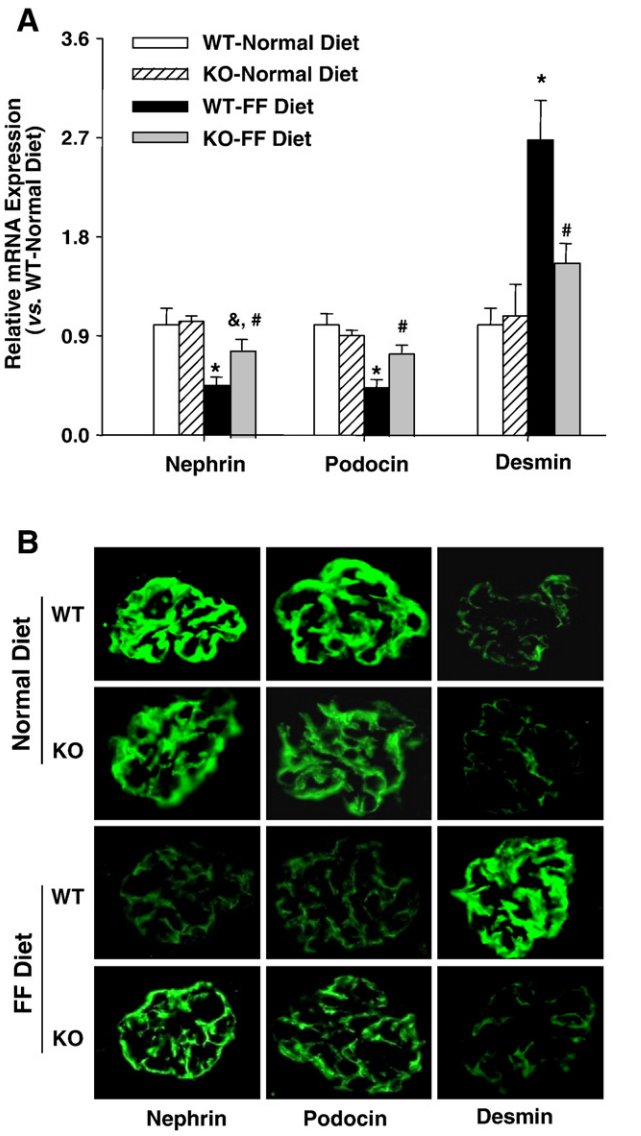

Fig. 5. Expression of nephrin, podocin, and desmin in gp91^{phox} KO and WT mice. (A) Real-time RT-PCR analysis of the expression of nephrin, podocin, and desmin in the glomeruli of gp91^{phox} KO and WT mice ($n=6$). (B) Immunofluorescent staining of nephrin, podocin, and desmin in the glomeruli of the four groups of mice ($n=4$). *$P<0.05$ vs WT mice on the normal diet; #$P<0.05$ vs WT mice on the FF diet; &$P<0.05$ vs KO mice on the normal diet.

section in WT and KO mice. Podocytes were identified by staining with an antibody against the podocyte-specific marker WT1. There were similar numbers of WT1-stained podocytes in WT and KO mice fed a normal diet. FF diet treatment induced a significant decrease in podocyte numbers in WT mice, but not in KO mice (Figs. 6B and 6C).

Blockade of Hcys-induced $O_2^{\bullet-}$ production by gp91^{phox} gene silencing in cultured podocytes

Although we have demonstrated in whole-animal experiments that the glomeruli of gp91^{phox} KO mice were protected from hHcys-induced renal injury, it has yet to be determined whether such protective action is due to the direct protection of podocytes. To address this issue and to explore potential underlying mechanisms, we used in vitro cultured podocytes to examine the role of gp91^{phox}-containing NADPH oxidase in Hcys-induced podocyte injury. Real-time RT-PCR showed that L-Hcys stimulated the expression of gp91^{phox} at both the mRNA and the protein level ($P<0.05$, Fig. 7A). This increased gp91^{phox} expression was accompanied by an elevated NADPH oxidase-dependent $O_2^{\bullet-}$ production (Fig. 7B). When podocytes were transfected with gp91^{phox} siRNA, Hcys-induced $O_2^{\bullet-}$ production was significantly inhibited, which was comparable to the inhibition by DPI, a NADPH oxidase inhibitor ($P<0.05$, Fig. 7C).

Blockade of Hcys-induced decrease in VEGF-A secretion in podocytes by gp91^{phox} siRNA gene silencing

As a functional parameter of podocytes, VEGF-A production was detected in podocytes under various conditions. Fig. 8A shows that the mRNA expression of VEGF-A was decreased by L-Hcys in a concentration-dependent manner. As shown in Figs. 8B and 8C, VEGF-A production and secretion were dramatically reduced by the treatment with L-Hcys ($P<0.05$), which was similar to the designated positive control, PAN. When gp91^{phox} siRNA was transfected to inhibit $O_2^{\bullet-}$ production via NADPH oxidase, Hcys-induced decrease in VEGF-A secretion was significantly restored ($P<0.05$). Similarly, inhibition of NADPH oxidase activity using DPI also recovered VEGF secretion in podocytes.

Discussion

The goals of this study were to determine whether podocytes are a direct target of hHcys and to investigate the role of NADPH oxidase-dependent $O_2^{\bullet-}$ production in hHcys-induced podocyte injury. Using an FF diet-induced hHcys animal model in gp91^{phox} gene-deficient mice and in vitro cultured podocytes, we clearly demonstrated that hHcys directly induces podocyte injury and depletion through gp91^{phox}-containing NADPH oxidase activation and $O_2^{\bullet-}$ production.

There is considerable evidence supporting the critical role of ROS, particularly $O_2^{\bullet-}$, in the pathogenesis of kidney diseases, such as diabetic nephropathy [28] and hypertension-related nephropathy [29]. Among various enzymes involved in the generation of ROS, NADPH oxidase is regarded as the main source of $O_2^{\bullet-}$ production.

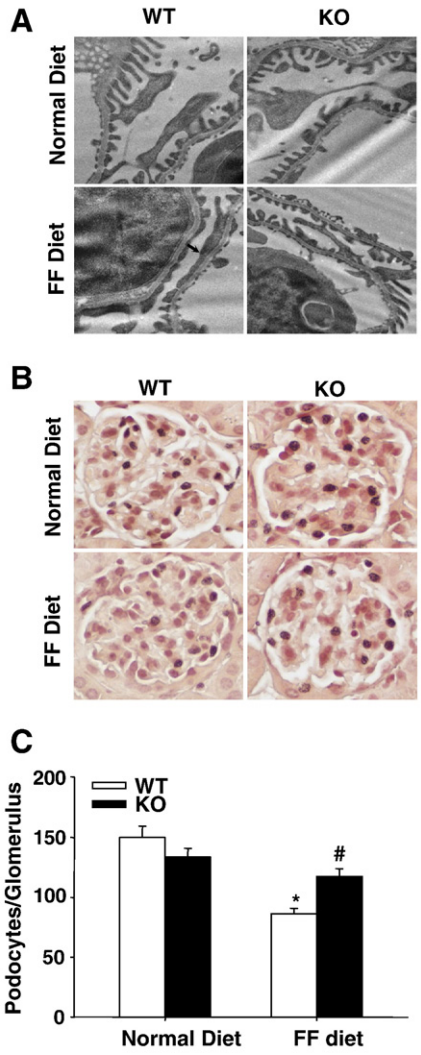

Fig. 6. Attenuation of foot process effacement and podocyte loss in the glomeruli of gp91^{phox} KO mice. (A) gp91^{phox} gene deletion improved podocyte ultrastructure in FF diet-treated mice. Arrow denotes the area of foot process effacement in WT mouse on the FF diet. Images are representative of six TEM images per kidney from three mice per group. Original magnification, ×8000. (B) Typical images of WT1-stained glomeruli from the four groups of mice (original magnification, ×400). (C) Summarized data showing podocyte numbers per glomerulus in each group ($n=6$). *$P<0.05$ vs WT mice on the normal diet; #$P<0.05$ vs WT mice on the FF diet.

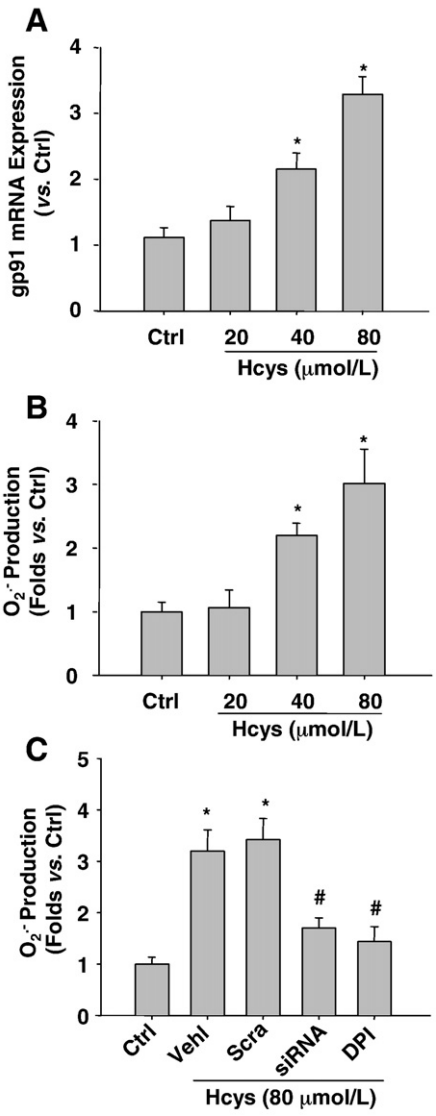

Fig. 7. L-Hcys increases gp91^{phox} expression and NADPH oxidase-dependent $O_2^{\cdot-}$ production in cultured podocytes. (A) L-Hcys stimulation for 12 h caused elevated gp91^{phox} mRNA expression in podocytes as determined by real-time RT-PCR ($n=4$). (B) ESR analysis shows that Hcys induces $O_2^{\cdot-}$ production in a concentration-dependent manner in podocytes ($n=5$). (C) ESR analysis shows that gp91^{phox} siRNA transfection or NADPH oxidase inhibition by DPI reduces $O_2^{\cdot-}$ production in podocytes. Ctrl, control; Vehl, vehicle; Scra, scrambled RNA; siRNA, gp91^{phox} siRNA ($n=6$). *$P<0.05$ vs control, #$P<0.05$ vs Hcys.

Gp91^{phox}, also known as NOX2, is the catalytic subunit of NADPH oxidase. Although there are some reports indicating that NOX1 and NOX4 are also expressed in the kidney [30,31], data from our laboratory and other groups have strongly suggested that the gp91^{phox}-containing NADPH oxidase system is more critical in mediating $O_2^{\cdot-}$ production in the kidney [4,10,11,32]. Therefore, we used gp91^{phox}-deficient mice to explore the role of NADPH oxidase-mediated $O_2^{\cdot-}$ production in hHcys-induced podocyte injury. It was found that the FF diet treatment increased plasma Hcys levels in both WT and KO mice, which indicates a successful establishment of the hHcys model and also suggests that gp91^{phox} itself is not involved in the metabolism of Hcys. Gp91^{phox} KO mice on the FF diet exhibited a lower level of renal $O_2^{\cdot-}$ production compared with WT mice, implying that gp91^{phox} gene deficiency prevents hHcys-induced local $O_2^{\cdot-}$ production in the kidney. In previous studies, gp91^{phox} KO mice have also been reported to have lowered $O_2^{\cdot-}$ production in many organs, such as the heart, lungs, and brain, which protects these mice from various pathophysiological conditions such as cardiac hypertrophy [8], hypoxic pulmonary hypertension [33], and surgically induced brain injury [34]. In accordance with lowered $O_2^{\cdot-}$ production in gp91^{phox} KO mice on the FF diet, urine albumin excretion in these mice was significantly decreased compared with WT mice on the same diet, suggesting that ROS-associated renal injury during hHcys is alleviated in these KO mice. Pathological studies using PAS staining showed that there was a significant improvement of hHcys-induced glomerulosclerosis in these KO mice compared with WT mice. Consistent with these pathological changes, GFR was also preserved in these KO mice on the FF diet. In addition, a 4-week FF diet treatment had no influence on arterial blood pressure of WT and gp91^{phox} KO mice, indicating that the preservation of podocyte function and structure in these KO mice is not associated with any change in blood pressure. All these results support the view that gp91^{phox}-containing NADPH oxidase mediates $O_2^{\cdot-}$ production in the glomeruli and thereby plays a critical role in hHcys-induced renal injury.

One of the most important findings of this study is that gp91^{phox} gene deficiency may protect podocytes from hHcys-induced injury.

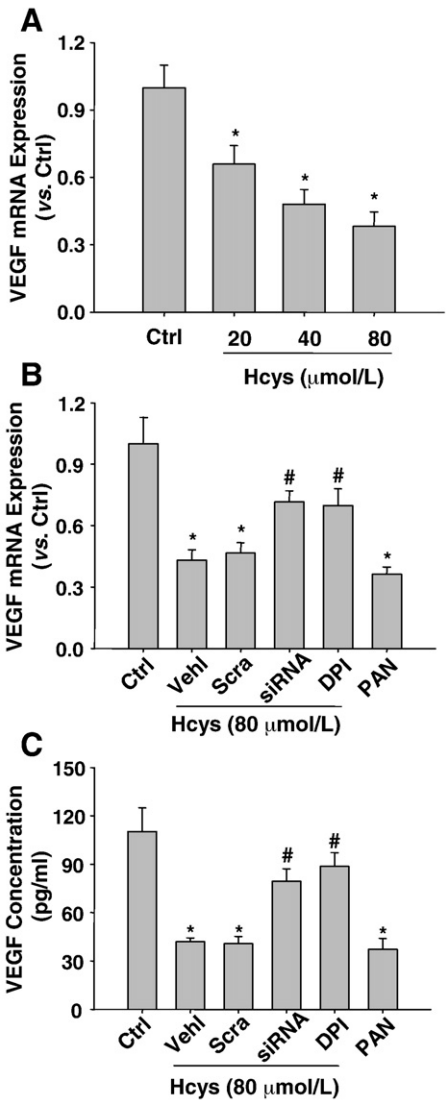

Fig. 8. Effects of gp91^{phox} gene silencing on L-Hcys-induced decrease in VEGF-A production and secretion in podocytes. (A) Real-time RT-PCR analysis shows that Hcys stimulation for 12 h decreases VEGF-A mRNA levels in a concentration-dependent manner ($n=4$). (B) Real-time RT-PCR analysis shows the expression of VEGF-A mRNA challenged by Hcys (80 μmol/L) for 12 h with various pretreatments. PAN was used as a positive control ($n=4$). (C) VEGF-A secretion in the culture medium detected by ELISA after pretreatment with various inhibitors and Hcys for 24 h. Ctrl, control; Vehl, vehicle; Scra, scrambled RNA; siRNA, gp91^{phox} siRNA ($n=5$). *$P<0.05$ vs control. #$P<0.05$ vs Hcys.

Podocytes serve as the final defense mechanism against urinary protein loss in the normal glomerulus [35]. Damage to podocytes and their slit diaphragm is intimately associated with proteinuria and glomerulosclerosis in many kidney diseases, such as focal segmental glomerulosclerosis, diabetic nephropathy, and hypertension-associated nephropathy [36,37]. In recent studies, we have reported that foot process effacement was presented in a methionine-induced animal model of hHcys [23], but the mechanism has not yet been explored. Here, we demonstrated for the first time that hHcys could induce podocyte injury through NADPH oxidase-mediated $O_2^{\bullet-}$ production, which was supported by analysis of the levels of some slit diaphragm molecules such as nephrin and podocin and by measuring the podocyte damage marker desmin. As is well known, nephrin and podocin are two important components of the slit diaphragm complex, which play an essential role in maintaining the normal structure of the glomerular filtration barrier. Mutation or down-regulation of these proteins is associated with a defective filtration barrier causing proteinuria [38]. In addition, nephrin affords important signaling cascades through its interaction with podocin and CD2-associated protein (CD2AP) for maintaining the normal growth of podocytes and preventing their apoptosis [38]. So, the decreased expression of nephrin is not only an indicator of slit diaphragm damage, but also a sign of a disturbed intracellular signaling pathway that is essential for podocyte survival. The results from this study show that hHcys induced a dramatic decrease in nephrin and podocin expression in WT mice, but not in gp91^{phox} KO mice. It seems that hHcys may disrupt the normal structure of the slit diaphragm complex and the related intracellular signaling events through NADPH oxidase-mediated $O_2^{\bullet-}$ production. This Hcys-induced podocyte injury and its attenuation in gp91^{phox} KO mice were also demonstrated by the increase in desmin expression. Desmin is an intermediate filament protein, which has long been suggested as a specific and sensitive podocyte injury indicator [7], and its expression is often up-regulated in various glomerular diseases in which podocyte damage is involved [18,39]. In this study, we showed that hHcys induced by the FF diet significantly increased desmin expression in the glomeruli of WT mice, but much less in gp91^{phox} gene KO mice, further suggesting that podocyte injury is significantly attenuated because of reduced $O_2^{\bullet-}$ generation in the kidney.

Among various morphologic characteristics, foot process effacement and consequent podocyte depletion are strong predictors for the progression of glomerulosclerosis. It has been proposed that the loss of <20% of podocytes triggers mesangial expansion, loss of 20–40% produces small patches of podocyte depletion and synechia formation, and >40% podocyte depletion produces the full picture of focal segmental glomerulosclerosis with segmental and eventually global sclerosis [40]. Although these observations identify podocyte depletion as one of the earliest cellular features of many types of kidney diseases, the mechanisms underlying the loss of podocytes remain poorly understood. Recently, it has been demonstrated ROS activation is a key mechanism leading to podocyte loss in animal models of diabetic nephropathy [13] and PAN-induced nephropathy [41]. In this study, the TEM data showed that FF diet treatment caused podocyte foot process effacement in WT mice, and such damage was dramatically attenuated in gp91^{phox} KO mice on the same diet. The fact that gp91^{phox} gene deletion provided protection from podocyte foot process effacement indicates that this podocyte injury is a direct action of hHcys on podocytes and it is through NADPH oxidase-mediated ROS toxicity. Using WT1 staining to calculate podocyte numbers and evaluate podocyte loss in the glomeruli, we found that hHcys significantly decreased podocyte numbers in the glomeruli of WT mice, indicating a podocyte loss under such pathological conditions. Interestingly, gp91^{phox} gene deletion prevented such podocyte loss induced by hHcys. These results suggest that the activation of NADPH oxidase and subsequent $O_2^{\bullet-}$ production is an important mechanism in mediating Hcys-induced podocyte injury and death. In harmony with our results, Liu et al. recently provided evidence showing that up-regulation of NADPH oxidase activity plays a pivotal role in mediating proximal tubular cell apoptosis in transgenic mice overexpressing angiotensinogen [42]. It should be noted that some previous studies reported the effects of hHcys in inducing renal cell proliferation through the activation of NADPH oxidase in other cell types such as mesangial cells [27]. It seems that the action of NADPH oxidase in causing cell proliferation or death may be cell-type specific. Although the function of NADPH oxidase-derived ROS in mediating renal cell proliferation and death seems to be paradoxical, these actions may eventually converge at the functional level, in that both processes may be detrimental (for example, proliferation of mesangial cells and depletion of podocytes) to normal kidney functions [43].

To address whether this protective effect of gp91^{phox} gene deletion is directly associated with counteracting Hcys-induced injury to

podocytes, we used cultured murine podocytes to examine the direct effects of gp91^{phox} gene silencing on Hcys-induced functional changes. It was found that Hcys induced an increase in the expression of gp91^{phox} and a dramatic enhancement of $O_2^{\bullet-}$ production in a concentration-dependent manner, which was blocked when podocytes were transfected with gp91^{phox} siRNA. These results provide evidence that Hcys is able to directly act on podocytes, initiating local oxidative stress and resulting in podocyte injury via activation of NADPH oxidase. In accordance with our findings, Eid et al. demonstrated that NADPH oxidase-dependent $O_2^{\bullet-}$ generation also mediates high-glucose-induced podocyte injury using the same cell line as we used [13]. There is also another study indicating that NADPH oxidase-mediated $O_2^{\bullet-}$ generation serves as the main mediator of PAN-induced podocyte damage [44]. It seems that NADPH oxidase-mediated $O_2^{\bullet-}$ production is an important detrimental factor in podocyte injury, which may initiate and promote glomerulosclerosis.

To further investigate the functional abnormality of Hcys-induced podocyte injury via NADPH oxidase activation, we examined the production of VEGF-A in cultured podocytes. In the kidney, VEGF-A is mainly derived from podocytes and regulates the cytoskeletal organization and migration of glomerular endothelial cells, facilitating the formation of a new vascular lumen [45]. A recent report has demonstrated that podocytes have a functional autocrine VEGF-A system, which is regulated by differentiation and ligand availability [46]. The function of VEGF-A in podocytes includes promoting cell survival through VEGFR2, inducing podocin up-regulation, and increasing nephrin/CD2AP interaction [46]. VEGF-A may also serve as a crucial growth factor in maintaining the normal function of podocytes by preventing their apoptosis through the interaction with nephrin and activation of the AKT signaling pathway [47]. Podocyte-derived VEGF-A is decreased in sclerotic glomeruli [48], whereas treatment with exogenous VEGF-A decreases renal sclerotic injuries and restores glomerular capillaries [49]. In this study, we found that Hcys treatment significantly decreased the production of VEGF-A in podocytes, which was restored by silencing of the gp91^{phox} gene or by inhibition of NADPH oxidase activity. It seems that elevated $O_2^{\bullet-}$ production induced by Hcys damages the normal function of podocytes to secrete this important growth and permeability factor in the glomeruli. Given the important role of VEGF in maintaining the normal function of podocytes and preventing their apoptosis, it is plausible that decreased nephrin expression, reduced VEGF excretion, and subsequent disturbed VEGF–nephrin interaction induced by hHcys may contribute importantly to Hcys-induced podocyte depletion.

In summary, this is the first report showing that Hcys may directly cause podocyte injury and depletion, which are important events leading to glomerulosclerosis associated with hHcys. Using a gp91^{phox} gene KO mouse model, we found that all hHcys-induced structural and functional changes reflecting podocyte injury were alleviated, such as proteinuria, reduced expression of podocin and nephrin, increased desmin level, foot process effacement, and podocyte loss. In cultured murine podocytes, we further demonstrated that silencing of the gp91^{phox} gene inhibited $O_2^{\bullet-}$ production induced by Hcys and recovered Hcys-induced decrease in secretion of VEGF-A. Collectively, these results demonstrate that a direct injurious effect of hHcys on podocytes is mainly mediated by a mechanism that involves generation of $O_2^{\bullet-}$ by the gp91^{phox}-containing NADPH oxidase, which may represent a specific early mechanism mediating hHcys-induced glomerulosclerosis.

Acknowledgments

This study was supported by Grants DK54927, HL075316, and HL57244 from the National Institutes of Health.

References

[1] Robinson, K.; Gupta, A.; Dennis, V.; Arheart, K.; Chaudhary, D.; Green, R.; Vigo, P.; Mayer, E. L.; Selhub, J.; Kutner, M.; Jacobsen, D. W. Hyperhomocysteinemia confers an independent increased risk of atherosclerosis in end-stage renal disease and is closely linked to plasma folate and pyridoxine concentrations. *Circulation* **94:**2743–2748; 1996.
[2] Moustapha, A.; Gupta, A.; Robinson, K.; Arheart, K.; Jacobsen, D. W.; Schreiber, M. J.; Dennis, V. W. Prevalence and determinants of hyperhomocysteinemia in hemodialysis and peritoneal dialysis. *Kidney Int.* **55:**1470–1475; 1999.
[3] Ducloux, D.; Motte, G.; Challier, B.; Gibey, R.; Chalopin, J. M. Serum total homocysteine and cardiovascular disease occurrence in chronic, stable renal transplant recipients: a prospective study. *J. Am. Soc. Nephrol.* **11:**134–137; 2000.
[4] Yi, F.; Li, P. L. Mechanisms of homocysteine-induced glomerular injury and sclerosis. *Am. J. Nephrol.* **28:**254–264; 2008.
[5] Griendling, K. K.; Minieri, C. A.; Ollerenshaw, J. D.; Alexander, R. W. Angiotensin II stimulates NADH and NADPH oxidase activity in cultured vascular smooth muscle cells. *Circ. Res.* **74:**1141–1148; 1994.
[6] Yi, F.; Zhang, A. Y.; Li, N.; Muh, R. W.; Fillet, M.; Renert, A. F.; Li, P. L. Inhibition of ceramide-redox signaling pathway blocks glomerular injury in hyperhomocysteinemic rats. *Kidney Int.* **70:**88–96; 2006.
[7] Sen, U.; Basu, P.; Abe, O. A.; Givvimani, S.; Tyagi, N.; Metreveli, N.; Shah, K. S.; Passmore, J. C.; Tyagi, S. C. Hydrogen sulfide ameliorates hyperhomocysteinemia-associated chronic renal failure. *Am. J. Physiol. Renal Physiol.* **297:**F410–F419; 2009.
[8] Deng, S.; Kruger, A.; Kleschyov, A. L.; Kalinowski, L.; Daiber, A.; Wojnowski, L. Gp91phox-containing NAD(P)H oxidase increases superoxide formation by doxorubicin and NADPH. *Free Radic. Biol. Med.* **42:**466–473; 2007.
[9] Gill, P. S.; Wilcox, C. S. NADPH oxidases in the kidney. *Antioxid. Redox Signaling* **8:** 1597–1607; 2006.
[10] Haque, M. Z.; Majid, D. S. Assessment of renal functional phenotype in mice lacking gp91PHOX subunit of NAD(P)H oxidase. *Hypertension* **43:**335–340; 2004.
[11] Haque, M. Z.; Majid, D. S. Reduced renal responses to nitric oxide synthase inhibition in mice lacking the gene for gp91phox subunit of NAD(P)H oxidase. *Am. J. Physiol. Renal Physiol.* **295:**F758–F764; 2008.
[12] Greiber, S.; Munzel, T.; Kastner, S.; Muller, B.; Schollmeyer, P.; Pavenstadt, H. NAD(P)H oxidase activity in cultured human podocytes: effects of adenosine triphosphate. *Kidney Int.* **53:**654–663; 1998.
[13] Eid, A. A.; Gorin, Y.; Fagg, B. M.; Maalouf, R.; Barnes, J. L.; Block, K.; Abboud, H. E. Mechanisms of podocyte injury in diabetes: role of cytochrome P450 and NADPH oxidases. *Diabetes* **58:**1201–1211; 2009.
[14] Whaley-Connell, A. T.; Chowdhury, N. A.; Hayden, M. R.; Stump, C. S.; Habibi, J.; Wiedmeyer, C. E.; Gallagher, P. E.; Tallant, E. A.; Cooper, S. A.; Link, C. D.; Ferrario, C.; Sowers, J. R. Oxidative stress and glomerular filtration barrier injury: role of the renin–angiotensin system in the Ren2 transgenic rat. *Am. J. Physiol. Renal Physiol.* **291:**F1308–F1314; 2006.
[15] Guo, J.; Ananthakrishnan, R.; Qu, W.; Lu, Y.; Reiniger, N.; Zeng, S.; Ma, W.; Rosario, R.; Yan, S. F.; Ramasamy, R.; D'Agati, V.; Schmidt, A. M. RAGE mediates podocyte injury in adriamycin-induced glomerulosclerosis. *J. Am. Soc. Nephrol.* **19:**961–972; 2008.
[16] Nagase, M.; Yoshida, S.; Shibata, S.; Nagase, T.; Gotoda, T.; Ando, K.; Fujita, T. Enhanced aldosterone signaling in the early nephropathy of rats with metabolic syndrome: possible contribution of fat-derived factors. *J. Am. Soc. Nephrol.* **17:** 3438–3446; 2006.
[17] Matsui, I.; Hamano, T.; Tomida, K.; Inoue, K.; Takabatake, Y.; Nagasawa, Y.; Kawada, N.; Ito, T.; Kawachi, H.; Rakugi, H.; Imai, E.; Isaka, Y. Active vitamin D and its analogue, 22-oxacalcitriol, ameliorate puromycin aminonucleoside-induced nephrosis in rats. *Nephrol. Dial. Transplant.* **24:**2354–2361; 2009.
[18] Zou, J.; Yaoita, E.; Watanabe, Y.; Yoshida, Y.; Nameta, M.; Li, H.; Qu, Z.; Yamamoto, T. Upregulation of nestin, vimentin, and desmin in rat podocytes in response to injury. *Virchows Arch.* **448:**485–492; 2006.
[19] Chen, Y. F.; Li, P. L.; Zou, A. P. Effect of hyperhomocysteinemia on plasma or tissue adenosine levels and renal function. *Circulation* **106:**1275–1281; 2002.
[20] Li, N.; Chen, L.; Yi, F.; Xia, M.; Li, P. L. Salt-sensitive hypertension induced by decoy of transcription factor hypoxia-inducible factor-1alpha in the renal medulla. *Circ. Res.* **102:**1101–1108; 2008.
[21] Zhang, G.; Zhang, F.; Muh, R.; Yi, F.; Chalupsky, K.; Cai, H.; Li, P. L. Autocrine/paracrine pattern of superoxide production through NAD(P)H oxidase in coronary arterial myocytes. *Am. J. Physiol. Heart Circ. Physiol.* **292:**H483–H495; 2007.
[22] Zhang, A. Y.; Yi, F.; Jin, S.; Xia, M.; Chen, Q. Z.; Gulbins, E.; Li, P. L. Acid sphingomyelinase and its redox amplification in formation of lipid raft redox signaling platforms in endothelial cells. *Antioxid. Redox Signaling* **9:**817–828; 2007.
[23] Yi, F.; dos Santos, E. A.; Xia, M.; Chen, Q. Z.; Li, P. L.; Li, N. Podocyte injury and glomerulosclerosis in hyperhomocysteinemic rats. *Am. J. Nephrol.* **27:**262–268; 2007.
[24] Iacobini, C.; Menini, S.; Oddi, G.; Ricci, C.; Amadio, L.; Pricci, F.; Olivieri, A.; Sorcini, M.; Di Mario, U.; Pesce, C.; Pugliese, G. Galectin-3/AGE-receptor 3 knockout mice show accelerated AGE-induced glomerular injury: evidence for a protective role of galectin-3 as an AGE receptor. *FASEB J.* **18:**1773–1775; 2004.
[25] Yang, L.; Zheng, S.; Epstein, P. N. Metallothionein over-expression in podocytes reduces adriamycin nephrotoxicity. *Free Radic. Res.* **43:**174–182; 2009.
[26] Zheng, S.; Carlson, E. C.; Yang, L.; Kralik, P. M.; Huang, Y.; Epstein, P. N. Podocyte-specific overexpression of the antioxidant metallothionein reduces diabetic nephropathy. *J. Am. Soc. Nephrol.* **19:**2077–2085; 2008.
[27] Yang, Z. Z.; Zou, A. P. Homocysteine enhances TIMP-1 expression and cell

proliferation associated with NADH oxidase in rat mesangial cells. *Kidney Int* **63:** 1012–1020; 2003.
[28] Susztak, K.; Raff, A. C.; Schiffer, M.; Bottinger, E. P. Glucose-induced reactive oxygen species cause apoptosis of podocytes and podocyte depletion at the onset of diabetic nephropathy. *Diabetes* **55:**225–233; 2006.
[29] Manning Jr., R. D.; Tian, N.; Meng, S. Oxidative stress and antioxidant treatment in hypertension and the associated renal damage. *Am. J. Nephrol.* **25:**311–317; 2005.
[30] Fujii, M.; Inoguchi, T.; Maeda, Y.; Sasaki, S.; Sawada, F.; Saito, R.; Kobayashi, K.; Sumimoto, H.; Takayanagi, R. Pitavastatin ameliorates albuminuria and renal mesangial expansion by downregulating NOX4 in db/db mice. *Kidney Int.* **72:** 473–480; 2007.
[31] Gorin, Y.; Block, K.; Hernandez, J.; Bhandari, B.; Wagner, B.; Barnes, J. L.; Abboud, H. E. Nox4 NAD(P)H oxidase mediates hypertrophy and fibronectin expression in the diabetic kidney. *J. Biol. Chem.* **280:**39616–39626; 2005.
[32] Yi, F.; Zhang, A. Y.; Janscha, J. L.; Li, P. L.; Zou, A. P. Homocysteine activates NADH/NADPH oxidase through ceramide-stimulated Rac GTPase activity in rat mesangial cells. *Kidney Int.* **66:**1977–1987; 2004.
[33] Liu, J. Q.; Zelko, I. N.; Erbynn, E. M.; Sham, J. S.; Folz, R. J. Hypoxic pulmonary hypertension: role of superoxide and NADPH oxidase (gp91phox). *Am. J. Physiol. Lung Cell Mol. Physiol.* **290:**L2–L10; 2006.
[34] Lo, W.; Bravo, T.; Jadhav, V.; Titova, E.; Zhang, J. H.; Tang, J. NADPH oxidase inhibition improves neurological outcomes in surgically-induced brain injury. *Neurosci. Lett.* **414:**228–232; 2007.
[35] Nagase, M.; Shibata, S.; Yoshida, S.; Nagase, T.; Gotoda, T.; Fujita, T. Podocyte injury underlies the glomerulopathy of Dahl salt-hypertensive rats and is reversed by aldosterone blocker. *Hypertension* **47:**1084–1093; 2006.
[36] Pavenstadt, H.; Kriz, W.; Kretzler, M. Cell biology of the glomerular podocyte. *Physiol. Rev.* **83:**253–307; 2003.
[37] Faul, C.; Asanuma, K.; Yanagida-Asanuma, E.; Kim, K.; Mundel, P. Actin up: regulation of podocyte structure and function by components of the actin cytoskeleton. *Trends Cell Biol.* **17:**428–437; 2007.
[38] Kawachi, H.; Miyauchi, N.; Suzuki, K.; Han, G. D.; Orikasa, M.; Shimizu, F. Role of podocyte slit diaphragm as a filtration barrier. *Nephrology (Carlton)* **11:**274–281; 2006.
[39] Lenz, O.; Elliot, S. J.; Stetler-Stevenson, W. G. Matrix metalloproteinases in renal development and disease. *J. Am. Soc. Nephrol.* **11:**574–581; 2000.
[40] Wharram, B. L.; Goyal, M.; Wiggins, J. E.; Sanden, S. K.; Hussain, S.; Filipiak, W. E.; Saunders, T. L.; Dysko, R. C.; Kohno, K.; Holzman, L. B.; Wiggins, R. C. Podocyte depletion causes glomerulosclerosis: diphtheria toxin-induced podocyte depletion in rats expressing human diphtheria toxin receptor transgene. *J. Am. Soc. Nephrol.* **16:**2941–2952; 2005.
[41] Xiao, H.; Shi, W.; Liu, S.; Wang, W.; Zhang, B.; Zhang, Y.; Xu, L.; Liang, X.; Liang, Y. 1,25-Dihydroxyvitamin D(3) prevents puromycin aminonucleoside-induced apoptosis of glomerular podocytes by activating the phosphatidylinositol 3-kinase/Akt-signaling pathway. *Am. J. Nephrol.* **30:**34–43; 2009.
[42] Liu, F.; Wei, C. C.; Wu, S. J.; Chenier, I.; Zhang, S. L.; Filep, J. G.; Ingelfinger, J. R.; Chan, J. S. Apocynin attenuates tubular apoptosis and tubulointerstitial fibrosis in transgenic mice independent of hypertension. *Kidney Int.* **75:**156–166; 2009.
[43] Jiang, F. NADPH oxidase in the kidney: a Janus in determining cell fate. *Kidney Int.* **75:**135–137; 2009.
[44] Marshall, C. B.; Pippin, J. W.; Krofft, R. D.; Shankland, S. J. Puromycin aminonucleoside induces oxidant-dependent DNA damage in podocytes in vitro and in vivo. *Kidney Int.* **70:**1962–1973; 2006.
[45] Munoz-Chapuli, R.; Quesada, A. R.; Angel Medina, M. Angiogenesis and signal transduction in endothelial cells. *Cell Mol. Life Sci.* **61:**2224–2243; 2004.
[46] Guan, F.; Villegas, G.; Teichman, J.; Mundel, P.; Tufro, A. Autocrine VEGF-A system in podocytes regulates podocin and its interaction with CD2AP. *Am. J. Physiol. Renal Physiol.* **291:**F422–F428; 2006.
[47] Foster, R. R.; Saleem, M. A.; Mathieson, P. W.; Bates, D. O.; Harper, S. J. Vascular endothelial growth factor and nephrin interact and reduce apoptosis in human podocytes. *Am. J. Physiol. Renal Physiol.* **288:**F48–F57; 2005.
[48] Yuan, H. T.; Li, X. Z.; Pitera, J. E.; Long, D. A.; Woolf, A. S. Peritubular capillary loss after mouse acute nephrotoxicity correlates with down-regulation of vascular endothelial growth factor-A and hypoxia-inducible factor-1 alpha. *Am. J. Pathol.* **163:**2289–2301; 2003.
[49] Kang, D. H.; Johnson, R. J. Vascular endothelial growth factor: a new player in the pathogenesis of renal fibrosis. *Curr. Opin. Nephrol. Hypertens.* **12:**43–49; 2003.